Vortex breakdown location over 65° delta wings empiricism and experiment

C. E. Jobe
Retired
Air Force Research Laboratory
Wright-Patterson AFB, Ohio, USA

ABSTRACT

Thirty-eight data sets from static tests of various 65° delta wings in many water and wind tunnels are compared with four empirical vortex breakdown location prediction methods and the results of two Navier-Stokes computations to assess their range of validity in pitch. Vortex breakdown is the sudden expansion and subsequent chaotic evolution of the otherwise orderly, spiraling, leading-edge vortex flow over the upper surface. Large fluctuations occur in vortex breakdown location at static test conditions making accurate experimental determination difficult.

The prediction methods do not account for the seemingly minor geometric details that vary between the models such as thickness, leading-edge bevel angle and radius, trailing-edge bevel angle, sting mounting, instrument housings, etc. These geometric variations significantly affect the position of vortex breakdown and degrade the accuracy of the predictions. The large changes in the flow produced by small geometric changes indicate that an efficient flow control strategy may be possible. Many of the data sets are not corrected for tunnel wall effects, which may account for some of the differences. Data presented herein are as published by the original authors, without additional corrections.

NOMENCLATURE

A	test conducted in air (Table 1) or empirical constant (Equation (1))
b	wingspan
B	wind-tunnel span
c	root chord
C	wind-tunnel throat area
M	Mach number
n	empirical exponent (Equation 1)
N-S	value computed using Navier-Stokes equations
Re	Reynolds number
s	wing planform area
t	wing thickness
$t.e.$	trailing edge
W	test conducted in water
x	streamwise co-ordinate along root chord
α	angle between freestream velocity and root chord (sting angle)
φ	circulation along vortex core (Equation (1))
Γ	sweep angle
Λ	roll angle

1.0 INTRODUCTION

Many investigations[1-21] have been conducted to elucidate the aerodynamic characteristics and flowfield, particularly vortex breakdown location, about delta wings with various sweepback angles. Vortex breakdown or bursting refers to the structural change from a strong, regular, tight spiral motion to a weaker, bulbous, chaotic turbulent motion and occurs in two forms — the most often occurring spiral form and the bubble (axisymmetric) ogival form. The spiral form executes two or three turns in direction opposite to the sense of the leading-edge vortex before dissipating into swirling, turbulent flow. The distance covered by the turns will be shown subsequently. The two forms of vortex breakdown were first shown by Lambourne and Bryer in Ref. 6. The location of breakdown is usually taken to be the sudden expansion of the core observed using smoke or natural condensation depending on the experimental conditions. The location is not precise due to oscillations along the vortex core and an average location determined from photographic or visual data is given. Vortex breakdown causes severe nonlinearities and discontinuities in the aerodynamic forces and moments that limit the maneuverability of fighter aircraft and can cause uncommanded, unforeseen responses, thus its import.

Paper No. 2775. Manuscript received 29 July 2002, accepted 19 April 2004.

https://doi.org/10.1017/S0001924000000294 Published online by Cambridge University Press

Table 1
Vortex breakdown location for 65° delta wings

Reference		Upper surface (leeward)	Lower surface (windward)	Trailing edge (t.e.)	t/c %	Reynolds no. (thousands)	Vortex breakdown $\alpha = 30°$, c
Huang & Hanff[1] 96	A	10° bevel	10° bevel	10° symm	1·53	3,600A body on	0·59
turbulence point	B	"	"	"	"	"	0·70
93	C	"	"	"	"	"	0·446
	D	flat prediction method					0·4253
Cipolla[2] 96		10° bevel	10° bevel	flat/flat	1·58	32·4W body on	0·29
Earnshaw[3] 65		cubic curve	symmetric	sharp	4·0	955A	0·45
Earnshaw & Lawford[4] 66	A	flat	cir.arc in x	shar	6·00	440.A	0·34
	B	cir. arc in x	flat	sharp	6·00	440.A	0·61
Guglieri *et a1*[5] 92	A	flat	30° bevel	flat/30"	2·35	295.A body on	0·12
	B	"	"		2·35	213.A body off	0·18
Lambourne & Bryer[6] 61	A	flat	16° chamfer	flat/16"	2·21	10.W	0·28E
	B	"	"	"	"	80.W	0·25E
	C	"	"	"	6·32	260.A	0·17E
	D	"	"		"	4,600.A	O.E
Lowson & Riley [7] 94	A	*repeat of L&B experiment ref. 6C*			6·29		0·28
	B	*repeat of W7K experiment ref. 13*			0·92		0:29
Panton[8] 90		flat	15° bevel	?	2·12	35.W	0·20
Pelletier[9] 94	A	10° bevel	10° bevel	10° symm	1·79	100.A body on	0·282
	B	flat	45° bevel	flat/flat	"	100.A body on	0·290
	C	10° bevel	10° bevel	10° symm	"	100.A body off	0·258
	D	flat	45° bevel	flat/flat	"	100.A body off	0·301
Skow & Erickson[10] 82	A	Fig. 15[10]	?	?	?	30.W	0·258
	B	Fig. 49[10]					0·308
Thompson[11] 75		15° chamfer	15° chamfer	30° symm	1·20	9·8W	0·307
Traub[12] 96		flat prediction method					0·142
Wentz & Kohlman[13] 69		7·5° chisel	7·5° chisel	15° symm	0·92	1,000A	0·218
Huang, Sun & Hanff 97a	1*	10° bevel	10° bevel	flat/flat	7·20	15.W	0.500
Ref. 14	4	flat	45° bevel	flat/45 deg bev	1·60	15:W	0·316
	5	45° bevel	flat	45° bev/flat	"	15:W	0·337
	6	flat	45° bevel	flat/45° bev	"	15.W bod on	0·335
	7	10° bevel	flat	10° bev/flat	"	15.W	0·428
	8	"	"	flat/flat	"	15.W	0·388
	9	"	"	"	"	15.W body on	0·428
	10	"	"	10° bev/flat	"	15.W	0·421
	11	"	"		"	15.W body on	0·45
	13	"	"	flat/flat	0·80	15.W	0·313
	14	flat	10° bevel	"	"	15.W	0·310
Huang, Sun & Hanff[15] 97b		flat	prediction method			0·338	
Traub[16] 97		flat	prediction method			0·226	
Verhaagen[17] 97		flat	30° bevel	flat/22° bev	3·0	2,300 A	0·20
Addington[18] 98		10° bevel	10° bevel	10° bev/10°	2·11	290.A body on	0·2310·25
Chaderjian & Schiff[19] 93		10° bevel	10° bevel	10° bey/10°	1·53	3,670 N-S	0·515
Gordnier[20] 97		10° bevel	10° bevel	10° bev/10 °	1·58	32. N-S	0·288
Gursul[21] 94		flat	45° bevel	flat/flat	7·6	100.A	0·29

A = air W = water E = extrapolated N S = Navier Stokes computation *Author's model number

The 65° delta wing in pitch and roll at high angles-of-attack was extensively tested by Huang and Hanff[1] and subsequently by Cipolla[2], Pelletier[9] and Addington[18] who used nearly identical models albeit at much lower Reynolds numbers (Re) based on root chord, c. A large difference in vortex breakdown location is evident when comparing the data of Cipolla[2] (Re = 32,400) for the nearly identical wing to that of Huang and Hanff[1] (Re = 3·6m) at zero roll angle (φ) and 30° sting angle (α). The vortex breakdown location found by Pelletier[9] (Re = 0·1) and Addington[18] (Re = 0·29m), also for a nearly identical wing, agrees with that found by Cipolla[2] and the Navier-Stokes computations of Gordnier[20] (Re = 32,000). Table 1, a survey of data and prediction methods for delta wings with 65° sweep with various sharp leading-edge bevels and centre bodies, of varying thickness and in various incompressible flows, shows that vortex breakdown is considerably nearer the apex (further upstream) than found in the experiments of Huang and Hanff[1]. This difference, 0·3c, exceeds the inherent uncertainty in experimental data due to the highly unsteady oscillation of vortex breakdown location that may amount to 0·2c under steady test conditions[1]. The objective here is to determine if correlations of published data can explain the differences in vortex breakdown location.

https://doi.org/10.1017/S0001924000000294 Published online by Cambridge University Press

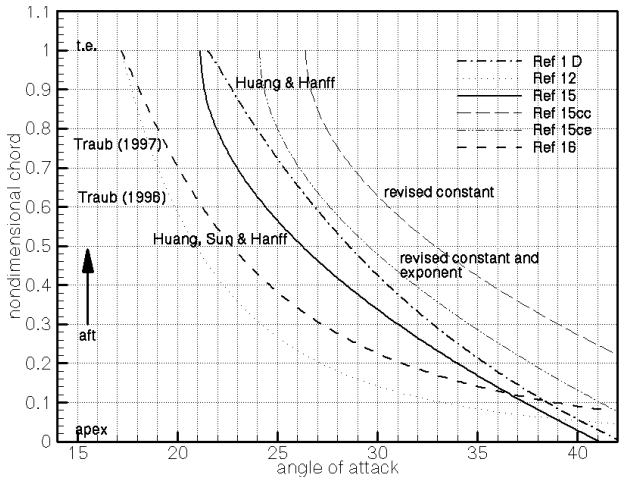


Figure 1. Empirical methods.

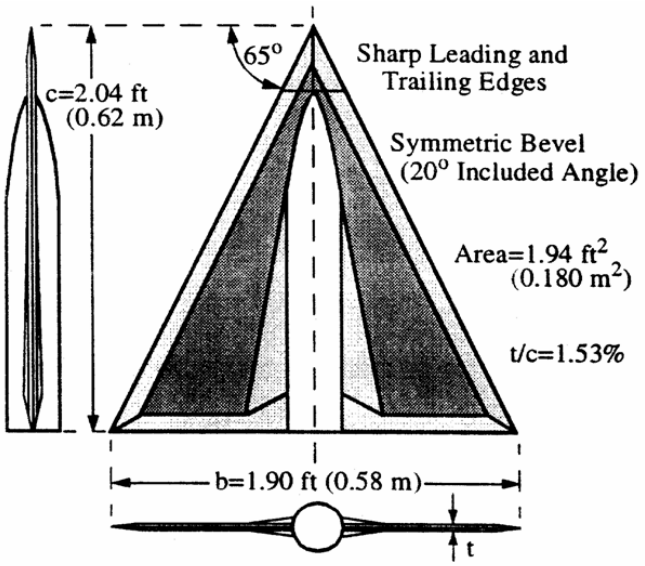


Figure 2. Huang and Hanff delta wing model.

2.0 COMPARISONS

Each data set is compared with four empirical methods; Huang and Hanff[1], Huang, Sun and Hanff[15], and two methods by Traub[12,16], shown in Fig. 1. The significant factors affecting the wing model and the experimental facility are discussed. Where multiple data sets are presented in one reference, they are distinguished by upper case letters. The details of each model and experiment are presented in Table 1. As shown, some investigators tested several geometric variations at multiple Reynolds numbers.

Initially, each experimental data set was separately compared to the four empirical methods shown in Fig. 1 to discern trends. This far exceeded the page limits. In this paper the data is grouped into five studies that pertain to: the Huang and Hanff model, the lower surface bevel effect, wall proximity and blockage effects, the double-bevel effect, the centrebody effect and miscellaneous data. The ratios of wingspan to tunnel span, b/B, and wing planform area to tunnel throat area, s/C are stated as percentages in parenthesis as each data set is introduced.

3.0 EMPIRICAL METHODS

The prediction method of Huang and Hanff[1] can account for pitch and roll changes on the static and dynamic vortex breakdown location of delta wings. The static prediction method shown as a heavy dot-dash line on Fig. 1 is based on an updated correlation of data from wings of sweeps from 55° to 80° from various facilities.

Huang, Sun and Hanff[15] revised their static vortex breakdown location prediction method using the wake circulation model suggested by Hemsch and Luckering[22], and by assuming a parabolic circulation distribution in the chord direction. A linear variation was used by Vissar and Nelson[23]. The constants in their quadratic equation for the circulation were '... determined iteratively on the basis of a large experimental database of breakdown locations for delta wings of different sweeps over a large range of angle-of-attacks. As a first approximation these quantities were found to be functions of sweep angle only ...' The predictions are generally aft (further from the apex) of the experimental data for wings with a flat upper surface.

The linear circulation, Γ, is given by:

$$\Gamma(x) = A\,(\mathrm{Sin}\alpha)^n\,(\mathrm{Tan}\Lambda)^{(2-n)}\,(\mathrm{Cos}\alpha)^{(1-n)}\,x/c \qquad \ldots (1)$$

where x is chord distance from the apex, A is an empirical constant, α is the angle-of-attack, Λ is the sweep angle, n is an empirical exponent and c is the root chord. Vortex breakdown occurs when the circulation attains a fixed, threshold value as suggested by Jumper, *et al*[24]. Huang, Sun and Hanff[15] used the values of the constant of $A = 4{\cdot}63$ and exponent, $n = 1{\cdot}2$, (shown as a heavy, solid line on Fig. 1) from Vissar and Nelson's[23] fit to circulation data for wing sweeps of 62, 70, 75, 80 and 85 degrees that includes Smith's thick conical wing theory estimate. Reducing A to 3·57 to fit experimental data however, places the predictions further aft (Fig. 1, curve 1*cc*) than all the experimental data herein. The values of $A = 3{\cdot}98$ and $n = 1{\cdot}27$ obtained by Visser and Washburn[25] as the best fit power curve to their wind tunnel circulation data for three wings with sweep angles of 70°, 76°, and 80° produces a similar aft shift. (Fig. 1, curve 1*ce*).

Traub[12], also used Equation (1) to develop the empirical vortex breakdown location prediction method shown as a heavy, dotted line on Fig. 1. He uses an exponential fit of experimental data (wing sweeps of 65°, 70° 75° and 80°) to determine the angle-of-attack at which vortex breakdown occurs at the trailing edge. The threshold value of the circulation at which vortex breakdown occurs, which is assumed constant for breakdown at any chord location, is determined using Equation 1. A circulation that varied with the one-third power of the chord distance was found to fit the experimental data.

The predictions are generally forward of the experimental vortex breakdown location. This prediction method fails to predict vortex breakdown reaching the apex due to the exponential decay to $\alpha = 90°$: however, the method is as accurate and nearly equal to the other methods at $\alpha = 0{\cdot}40°$ as shown on Fig. 1.

Traub's[16] revision of his earlier method[12], shown as the heavy, dashed line on Fig. 1, predicts vortex breakdown further aft for the same angle-of-attack at which vortex breakdown crosses the trailing edge, thus improving agreement with many sets of experimental data. The revision also uses Equation 1 and assumes a square root variation of the threshold value of circulation for vortex breakdown with cord distance and a linear variation of circulation with chord distance. The use of an experimentally determined point at which vortex breakdown crosses the trailing edge to start the calculation, instead of the suggested correlation, Equation (3) in Ref. 12, also improves the predictions, however the correlation was used here.

https://doi.org/10.1017/S0001924000000294 Published online by Cambridge University Press

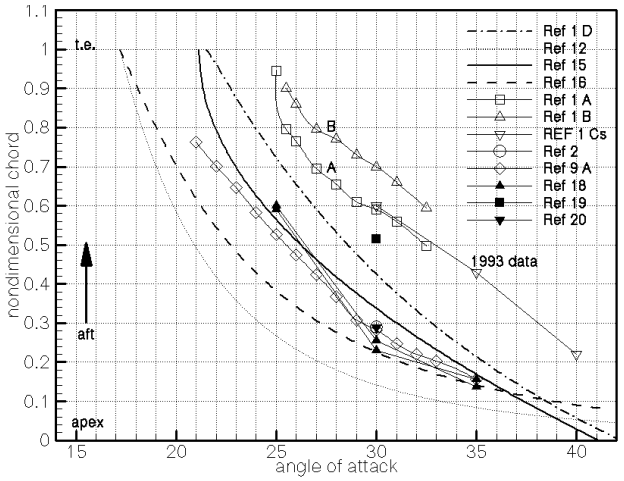


Figure 3. Huang and Hanff model data.

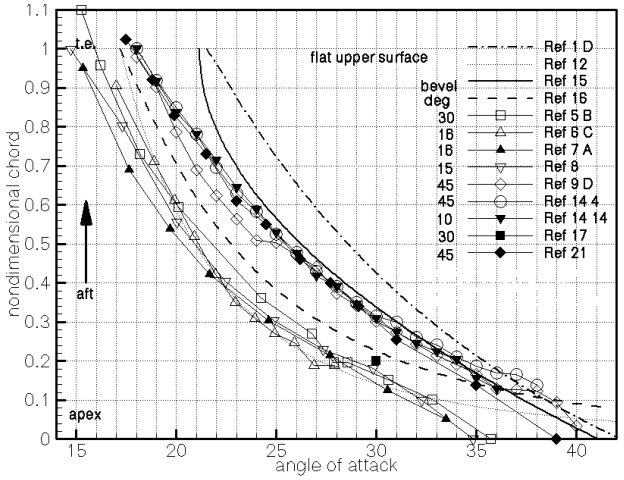


Figure 4. Lower surface bevel data.

3.1 Huang and Hanff model

The Huang and Hanff[1] model is shown in Fig. 2. It has been tested by Huang and Hanff in two wind tunnels (the Canadian Institute for Aerospace Research 6ft × 9ft and the Wright Laboratory 7ft × 10ft Subsonic Aerodynamic Research Laboratory). A facsimile of the model has been tested by Chipolla[2] in the Fluid Mechanics Laboratory of Lehigh University free-surface water channel (1m wide by 53cm deep at 17·8cms^{-1}) and by Pelletier[9] (4·3ms^{-1}) and separately by Addington[18] (14·7ms^{-1}) in the indraft subsonic wind tunnel (0·6m × 0·6m) at the University of Notre Dame. Navier-Stokes computations have been performed by Gordnier[20] (laminar) and Chaderjian and Schiff[9] (turbulent) to agree with the test conditions of Chipolla[2] and Huang and Hanff[1], respectively.

Figure 3 shows vortex breakdown location for the range of angle-of-attack when vortex breakdown is located above the wing's surface. At lower angles of attack, the leading edge vortex breaks down in the wake and at higher angles of attack the flow over the upper, leeward surface is fully separated and the vortex does not exist.

The higher Reynolds number data of Huang and Hanff[1] (b/B = 27·2%, s/C = 3·13%) is considerably aft (at about 0·6 chord versus about 0·3 chord for $\alpha = 30°$) of the prediction methods and the lower Reynolds number data that generally follows the prediction method of Huang, Sun and Hanff[15]. Huang and Hanff[1] attributed the difference to the slope of the bevelled upper surface in the freestream direction when the centreline is at zero angle-of-attack, corresponding to a flat upper surface. The 10° bevelled upper surface would attain zero angle-of-attack when the centreline is at 4·262°. Thus a 4° angle-of-attack correction due to leading edge bevel was proposed that brought the Huang and Hanff[1] data into closer agreement with the predictions. The 4·26° shift has been removed from the three 1993 data points shown.

The 10%c difference in location between the initial breakdown point (line A) and the turbulence point (line B) quantitatively illustrates the effect of a change in the definition of vortex breakdown location. Point A is the initial, abrupt kink in the observed vortex core where usually a reverse helix forms and continues downstream for approximately three turns before expanding into diffuse turbulence (point B). The spiral breakdown is usually observed with delta wings although the bubble type breakdown (sudden axisymmetric expansion of the leading-edge vortex core) has been observed on the same wing at the same time (Fig. 4, Ref. 6) at low Reynolds number (10,000).

The delta wing of Cipolla[2] (b/B = 18·9%, s/C = 3·62%) was modeled after that of Huang and Hanff[1] with a root chord of 8in vice their 24·485in. The trailing edge of Chipolla's model was blunt vice the 10° symmetrical bevel of Huang and Hanff[1], otherwise the models are identical. Chipolla's experiments, conducted in water at the Reynolds number of 32,400, studied the effect of roll angle at a constant sting angle of 30°, thus the single point at zero roll angle. Vortex breakdown was visualised by injection of dye from ports on the upper surface near the apex. The average (mean of ten readings over 20s at a reduced frequency of 0·58: free stream at 17·8 cms^{-1} and root chord of 203mm) vortex breakdown location was recorded as a function of roll angle for steady-state and forced oscillatory conditions. Vortex breakdown location data versus roll angle for fixed sting angle is not as available as pitch data. Chipolla's[2] single data point at $\alpha = 30°$, Fig. 3, falls closer to the predictions of Huang, Sun and Hanff's[15] method and in between the predictions using Huang and Hanff's[1] older method and Traub's[16] method.

The data of Addington[18], (b/B = 46·44%, s/C = 11·57%) and Pelletier[9], taken in the same wind tunnel on very similar models, are in close agreement - within the experimental error given by Addington, ±0·3° in roll angle and ±0·5° in sting angle. Addington's Reynolds number increase of 290% is due to the use of a different model and a velocity increase of 342%. Pelletier studied the centre-body effect and his data will be discussed subsequently in that section. Addington[18] presented two sets of vortex breakdown location data, one for each half of the wing, indicating an asymmetry due to model construction imperfections between the port and starboard halves and/or misalignment in roll and/or yaw angle with the freestream. Since the relative forward and aft positions of the vortex breakdown location switches from starboard to port at about 33° angle-of-attack, Fig. 3, misalignment with the freestream is indicated.

Two separate computations using the Navier-Stokes equations have been performed by Chaderjian and Schiff[19] and Gordnier[20]. The flow conditions considered by Chaderjian and Schiff (Re = 3·67 million, M = 0·27) correspond to the experiments of Hanff and Huang[1] and their predicted vortex breakdown location is at 0·515 chord, interspersed with the experimental data, on Fig. 3. The computations of Gordnier[20] were performed at nearly the same Reynolds number (32,000) as the experiments of Cipolla[2] although at a higher Mach number (0·2). His results for vortex breakdown location (28·8% chord) are in nearly exact agreement with the experimental data (29% chord) shown on Fig. 3.

3.2 Lower surface bevel effects

The geometric and flow data for each flat upper surface wing are shown in Table 1. The vortex breakdown location data are shown in Fig. 4. For the 65° delta wing, the predictions of Traub[12] agree with

https://doi.org/10.1017/S0001924000000294 Published online by Cambridge University Press

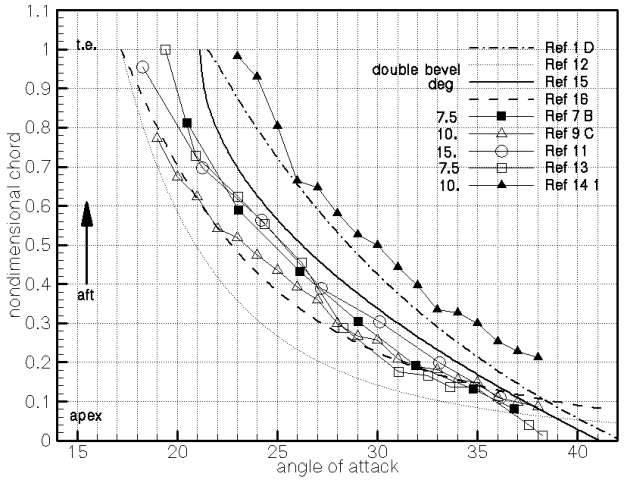


Figure 5.

the flat upper surface data, except Pelletier's[9], Huang, Sun and Hanff's[14], and Gursul's[21].

Although a wide range of Reynolds numbers is included (15,000 to 2·3m and the data of Lambourne and Bryer[6], is representative of their data at 4·6m), all of the data is further forward than the high Reynolds number (3·6m) data of Huang and Hanff[1], Fig. 1. Comparison of Huang, Sun and Hanff's[14] and Gursul's[21] data with the data of Pelletier (Ref. 9 D) for his 45° lower surface bevel on the leading edges only (blunt trailing edge) shows agreement over the forward 50% chord and an upstream shift of about 8% chord to the 90% chord station followed by close agreement to the trailing edge. However, with the exception of Huang, Sun and Hanff's[14] data for the 10° bevel, increasing lower surface bevel moves vortex breakdown location aft, indicating a weaker vortex.

Gursul[21] (b/B = 42·6%, s/C = 8·5%) The vortex breakdown location data for this thick wing (7·6%) agrees with the Huang, Sun and Hanff[14] data up to 30° angle-of-attack then deviates upstream by 5-10% as vortex breakdown approaches the apex. This data does not show the upstream shift as in Pelletier's[9] data at the same Reynolds number and is in closer agreement with the low Reynolds number data of Huang, Sun and Hanff[14]. Here the effects of thickness appear negligible except when vortex breakdown is very near the apex, contrary to the 10% upstream shift found by Huang, Sun and Hanff[14] (Wings 8 and 13) for an upper surface bevel of 10°, flat lower surface.

Lambourne and Bryer[6] (b/B = 61%, s/C = 25·92%) following measurements in the vortex flow generated by a 65° delta wing at α = 15°, tested a series of swept plates and flat plate delta wings bevelled at 16° on the lower surface only; in both water and wind tunnels. The wings were tested plain and modified by the addition of wire, spoilers and fairings to test possible influences on the vortex burst position. None of the additions had a significant effect. The authors attribute the downstream shift (for the higher angles-of-attack above where breakdown crosses the trailing edge which is at the same angle-of-attack ≈ 16°) at the lowest Reynolds number to a genuine Reynolds number effect since the data at 10,000 and 80,000 were taken in the same water tunnel with the same model, varying the speed from 2ins^{-1} to 16ins^{-1}. The data at Re = 80,000 and 260,000 closely agrees even though the thickness changed from 2·21% to 6·32%, indicating little effect of thickness or Reynolds number above 80,000. The ratio of the wingspan to the relevant tunnel dimension also changed from 61% (the highest value used in any of the tests) to 41%. The data of Lambourne & Bryer[6] for their 16° chamfer on the leading-edge lower surface model follows the data of Guglieri and Quaglotti[5] and, with the exception of the lowest Reynolds number data (10,000), c1osely agrees with the predictions of Traub[12].

Lowson and Riley[7] (b/B = 35·2%, s/C = 8·86% and b/B = 31·71%, s/c = 7·19%) also noted the wide variations in the vortex breakdown location for wings of equal sweep among previous investigators' data and repeated the experiments of Lambourne and Bryer[6] and Wentz and Kohlman[13] at the original, quoted Reynolds numbers over a larger range of angle-of-attack. Their new data, in general, agrees with the previous data as shown in Fig. 4 and Fig. 5 and again shows vortex breakdown to be upstream of the location found by Huang and Hanff[1] and in agreement with Cipolla[2] and Pelletier[9]. The new experiments of Lowson and Riley[7] agree with the Wentz and Kohlman[13] data, Fig. 5, closer than with the older Lambourne and Bryer[6] data, Fig. 4. The authors successfully reproduced previously published results by using models of the exact geometry used in the prior investigations and concluded that variation of vortex breakdown position is principally due to changes in detail model geometry, particularly near the apex. The effects of geometric variations 'far outweigh those due to support interference, methods of flow visualisation, wind tunnel factors, and changes in Reynolds numbers.'

Verhaagen[17] (b/B = 34·44%, s/C = 9·88%) performed detailed measurements of the forces, moments, surface pressures and flow visualisation, both on and off the surface, in the low-turbulence-tunnel of the low-speed wind tunnel laboratory of the Delft University of Technology. The tests, conducted at 50ms^{-1}, corresponding to a Reynolds number of 2·3m, examined the effect of sideslip at a fixed sting angle of 30°. The relevant vortex breakdown location at zero sideslip is at x/c = 0·2.

The experiments of Panton[8] (b/B = 35%, s/C = 14·57%) clearly demonstrate some repeatability problems associated with vortex breakdown data. Three separate curves with an angle-of-attack scatter of about 2° were obtained because the same model was removed and reinstalled in the same water channel a year apart. These results apparently contradict the previous findings of Lowson and Riley[7]. The data selected by Panton to represent the three sets for additional comparisons agrees with the prediction method of Traub[12] perhaps due to the flat upper surface and 15° lower surface bevel. Here Re = 35,000, which is between Re = 10,000 and Re = 80,000, where Lambourne and Bryer[6] noted a downstream shift in vortex breakdown location due to Reynolds number.

A bevel on the lower surface produces a negative, conical camber along the entire leading edge which moves vortex breakdown location aft, increasing with increasing bevel angle. The Earnshaw and Lawford[4] and Lambourne and Bryer[6] data similarly show an aft movement of vortex breakdown location with positive, conventional camber. The data shown in Fig. 4 does not display a monotonic order based on bevel angle. Removing the effect of upper surface bevel or slope by considering only wing models with flat upper surfaces and lower surface bevel does not produce a correlation. Unfortunately, enough of these wings were not tested inverted to provide a similar comparison for upper surface bevelled, lower surface flat.

3.3 Wall proximity and blockage effects

The effects of wind tunnel wall proximity and blockage can be examined. For the flat upper surface wings, the upper surface bevel angle is also removed as a variable. The blockage is nearly the planform area/throat area, s/C, multiplied by the trigonometric Sin of the sting angle or α for moderate and high angles. There does not appear to be a correlation or trend with either blockage or wall proximity for the ranges of these variables encountered during these experiments.

3.4 Double bevel effects

Thompson[11] (b/B = 56%, s/C = 16·79%) conducted low Reynolds number water tunnel tests of a series of wings of various sweeps and cambers. This data set is most closely predicted by the method of Huang, Sun and Hanff[15] at the higher angles of attack while the

https://doi.org/10.1017/S0001924000000294 Published online by Cambridge University Press

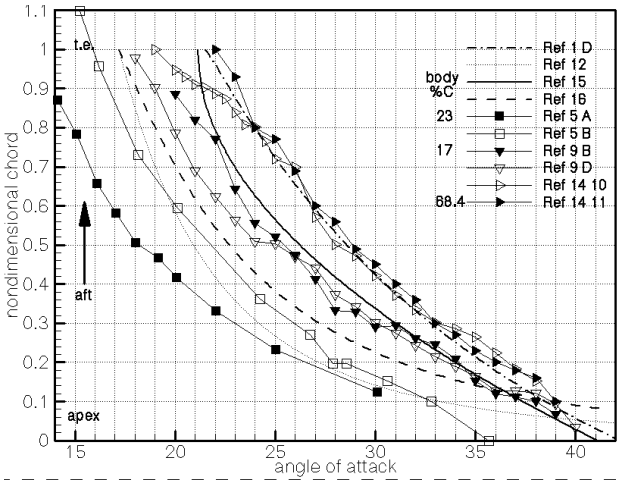


Figure 6. Centrebody effects.

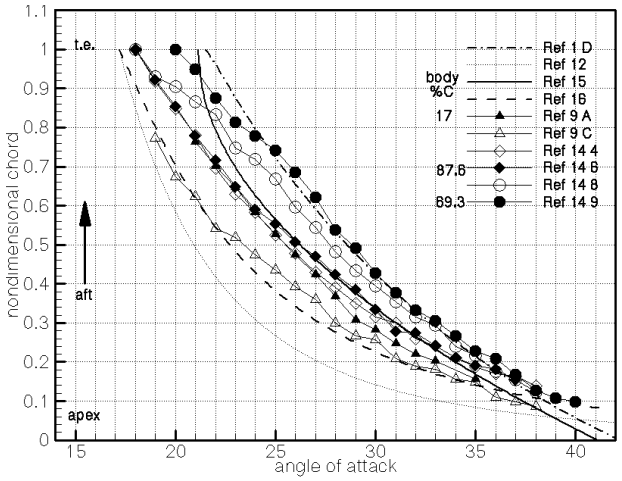


Figure 7. Centrebody effects (cont).

data approaches the predictions of Traub's[12] method when vortex breakdown is near the trailing edge ($a \approx 18°$).

Wentz and Kohlman[13] (b/B = 20·8%, s/C = 3·10%) performed a definitive set of experiments at Re = 1m on wings of many sweep angles. Data for the 65° delta wing lies upstream (forward) of the predictions using Huang, Sun and Hanff[15] method and downstream (aft) of the predictions using Traub's[12] method.

3.5 Centrebody effects

The six data sets shown in Fig. 6 and Fig. 7 specifically address the effect of a centre body: Guglieri *et al*, Huang, Sun and Hanff[14] (three sets) and Pelletier[9] (two sets). With the exception of the Guglieri *et al*[5] data, the addition of a centrebody moves vortex breakdown location aft along the wing chord. The aft movement is small throughout the angle-of-attack range and more pronounced at the trailing edge in most cases. The aft movement is more pronounced if the wing upper surface is bevelled.

Guglieri and Quagliotti's[5] (b/B = 26·4, s/C = 4·77) 2·35% thick delta wing had a small fuselage (a housing for force and pressure instrumentation) on only the lower surface which was bevelled at 30°. The upper surface was flat. The fuselage consisted of a semicircular section (about 10% span in diameter) capped by an ogival nose shape attached to the lower surface about 25% of the root chord aft of the apex. The effect of the fuselage was determined by comparison with the data from two series of flat delta wings tested in the same wind tunnel at different Reynolds numbers (295,000 fuselage on vice 213,000 fuselage off) and the data of Skow and Erickson[10] and Wentz and Kohlman[13]. The addition of this small fuselage on the lower surface moves vortex breakdown toward the apex (upstream) at all angles of attack. The forward movement diminishes with angle-of-attack: from 30% chord at α = 16° to 4% chord at α = 30°. Vortex breakdown is nearer the apex than predicted by the method of Traub[12] with the fuselage on and intersects the predictions of Traub[12] with the fuselage off. Both data sets are considerably forward of the location predicted using the method of Huang, Sun and Hanff[15]. If considered as an angle-of-attack correction, on the average vortex breakdown occurs at the same chord location when,

$$\alpha_{fus\ off} - 2{\cdot}57° = \alpha_{fus\ on}$$

This correction is not constant with α; it decreases as α increases.

The addition of the fuselage on the lower surface produced an effective negative camber over the wing area occupied and thus moved the vortex breakdown location upstream, toward the apex.

Pelletier[9] (b/B = 54·4%, s/C = 15·87%) tested a family of delta wings designed to investigate the effects of the centrebody (a small, symmetrically-disposed top and bottom, housing for the instrumentation and mounting to the sting) and bevel angle on a 65° delta wing model patterned after that of Huang and Hanff. The single-bevel wing has a flat upper surface and a 45° bevel on the lower surface. The double-bevel wing has a symmetric 20° bevel identical to the wing tested by Huang and Hanff[1]. His data for the four geometric variations tested; centrebody on and off for both wings, at the Reynolds number of 100,000 lies between the predictions using the method of Traub[16] and the method of Huang, Sun and Hanff[15]. When vortex breakdown is near the apex all data and predictions tend to agree (about 38° angle-of-attack). Contrary to the upstream shift (toward the apex) of vortex breakdown found by Guglieri and Quagliotti[5] for the fuselage on the lower surface only, Pelletier[9] found that the addition of the symmetrically-disposed centrebody moved vortex breakdown downstream toward the trailing edge on both the single bevel and double bevel wings. The downstream shift diminishes as angle-of-attack increases and vanishes for the single bevel wing for $\alpha \geq 26°$. The average angle-of-attack correction for the double bevel wing, as computed here is:

$$\alpha_{fus\ off} + 1{\cdot}64° = \alpha_{fus\ on}$$

The symmetric bevel shifts vortex breakdown upstream toward the apex compared to the single bevel for the wings alone but has little or no effect with the centrebody on. Vortex breakdown over the single bevel (flat upper surface) wing is slightly forward of the predictions using Huang, Sun and Hanff's[15] method and aft of the predictions using Traub's[12] method, contrary to the flat upper surface wing data of Guglieri and Quagliotti[5], Lambourne and Bryer[6], and Panton[8] that tends to agree with the predictions of Traub's[16] method. When considering an angle-of-attack shift to account for the upper surface bevel versus a flat upper surface, the 4° correction, based on geometry, is excessive. From the wing alone data, this shift amounts to 1° or 2°

$$\alpha_{flat\ upper\ surface} = \alpha_{bevelled} + (1\ ° \text{ or } 2°)$$

and varies with α; not fixed at 4° for all α as proposed The correction vanished when the centrebody was added during this set of experiments.

A larger body effect was found by Pelletier[9] (body origin at 17%c) and Guglieri *et al*[5] (body origin at 23%c) because the body originated much further forward on the wing than in the experiments of Huang, Sun and Hanff[14] (69%c – 73%c).

https://doi.org/10.1017/S0001924000000294 Published online by Cambridge University Press

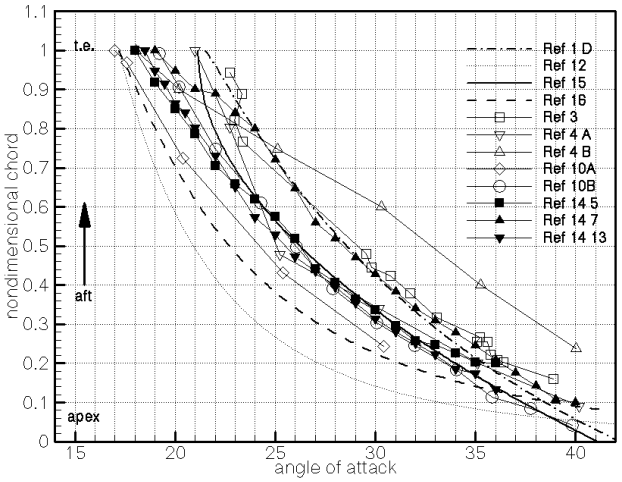


Figure 8. Miscellaneous data.

4.0 MISCELLANEOUS DATA

Earnshaw[3] (b/B = 35%, s/C = 8·49%) used the abrupt disappearance of density gradients near the vortex axis, as shown by a Schlieren system, to identify vortex breakdown. His data, at Re = 1m for a 4% thick symmetric wing with sharp edges and a chord section defined by a cubic curve, agrees with the older prediction method of Huang and Hanff[1], Fig. 8.

The 18in centreline chord model was tested at 100fts^{-1}. Distributed roughness was applied to the forward upper surface along with roughness strips located to move the 'kink' in the secondary separation line (indicating laminar to turbulent secondary separation) to the apex of each model tested. Tunnel constraint angle-of-attack corrections were applied.

Earnshaw and Lawford[4] (b/B = 20·1%, s/C = 2·89%) found the position at which the tightly-rolled leading-edge vortex breaks down to form a much more diffuse vortex by using a fine tuft at the end of a rod inserted through the tunnel wall. Subsequently, Earnshaw[3] found that 'introduction of the tuft-probe moved the breakdown position by 10-15% of centreline chord forward of the position given by the Schlieren system alone.' The 6% thick model had one flat side and one convex side generated by straight lines drawn from the tips to the circular-arc centreline section. The shift in vortex breakdown location due to camber is substantial: about 20% chord upstream when the upper surface is flat (negative camber). The root chord of this 65° delta wing was 0·8626ft based on the stated area of 0·347ft^2. This yields a Reynolds number of 0·44m based on the wind speed of 80fts^{-1} and standard atmospheric conditions. Tests at twice the wind speed showed no change in the breakdown point. A trend for the rapid rise of normal-force fluctuation to occur when the vortex breakdown is close to the trailing edge was noted. The surface oil flow photographs and topologies sketched in this report form the basis of many current papers. The data for the flat upper surface position follows the predictions of the Huang; Sun and Hanff[15] method while the data for the flat surface windward (lower) do not, Fig. 8.

Skow and Erickson[10] did not state the geometric data for their models in the reference. The vortex breakdown location given in these authors' Fig. 15 lies considerably upstream, nearer the apex, than the data for their delta wing with flaps set at 0 (their Fig. 49). The flapped delta wing data (from Fig. 49) agrees with the predictions using the method of Huang, Sun and Hanff[15] while the data from Fig. 15 lies between these predictions and those using Traub's[16] method, Fig. 8. The data were recorded in the Northrop water tunnel at a Reynolds number of 30,000 between the Reynolds numbers of 10,000 and 80,000 where Lambourne and Bryer[6] noted a Reynolds number effect.

Huang, Sun and Hanff[14] (b/B = 31·1%, s/C = 3·89%) tested a family of 20 delta wings in the Institute for Aerospace Research 15 × 20in free-surface water tunnel at Re = 15,000 based on the 5in root chord models. Eleven wings were swept 65°. The author's model number designation is retained and each model is discussed in relation to related experiments.

Wing 1. Fig. 5. This model is bevelled 10° on the windward and leeward leading edges as is their original wind-tunnel model. This is a blunt trailing-edge model without a fuselage or instrumentation housing, however. Although this model is 7·2% thick vice 1·53% and the Reynolds number is 15,000 vice 3,600,000, the vortex breakdown location falls forward of their previous (1993 and 1996) wind-tunnel data and lies just aft of the original Huang and Hanff[1] method predictions.

Wing 4. Fig. 4. Both this model and Pelletier's[9] model D and Gursul's[21] model have a flat upper surface and a 45° bevel on the lower, windward surface along the leading edges. The trailing edge of Pelletier's and Gursul's model is blunt vice bevelled. There is reasonably good agreement between the data sets even though the Reynolds number differs (Pelletier and Gursul tested in air at Re = 100,000 vice 15,000 in water). The data sets are in agreement with the predictions of the Huang, Sun and Hanff[5] method forward of 50% chord. The data of Pelletier lies upstream of both the predictions and water-tunnel data for $0{\cdot}5 \sim X/C \sim 0{\cdot}9$, however the data sets agree at the trailing edge.

Wing 5. Fig. 8. This is Wing 4 inverted. There is very little difference in the data thus causing questions on the effect of bevel on vortex breakdown at this low Reynolds number of 15,000.

Wing 6. Fig. 7. This is Wing 4 with a symmetrically-disposed centrebody similar to that on the Huang and Hanff[1] wind tunnel model but located 0·876c downstream of the wing's apex. The effect of the addition of the fuselage is very small or negligible, contrary to the effects found by Guglieri and Quagliotti[5] (an upstream movement of vortex breakdown) and Pelletier[9] (a downstream movement of vortex breakdown). The change in vortex breakdown position was determined by Guglieri and Quagliotti by comparison with other delta wings tested in the same wind tunnel at different Reynolds numbers where here care was taken to test the centrebody-on and centrebody-off models at identical conditions in sequence. The data agrees with the predictions of the Huang, Sun and Hanff[15] method for $0{\cdot}2 \le x/c \le 0{\cdot}6$.

Wing 7. Fig. 8. This data, for a wing bevelled at 10° on all upper, or leeward, surfaces and flat on the lower surfaces agrees with the original Huang and Hanff[1] prediction method that locates vortex breakdown downstream (further aft) than most data and prediction methods, except the high Reynolds number wind tunnel data of Huang and Hanff[1].

Wing 8. Fig. 7. The change from Wing 7 is the blunt (flat/flat) trailing edge that moves vortex breakdown 5-10% upstream (forward) along the entire wing chord. The effect is less pronounced forward of the half chord point. This data tends to agree with the prediction method of Huang and Hanff[1] for $x/c \le 0{\cdot}3$ and tends toward the predictions of Traub's[16] method near the trailing edge.

Wing 9. Fig. 7. The addition of a fuselage to Wing 8 moves vortex breakdown downstream 5-10% for $x/c \ge 0{\cdot}5$, i.e., on the aft part of the wing, bringing it into close agreement with the Wing 7 data. This data closely follows the prediction method of Huang and Hanff[1] for $x/c \le 0{\cdot}8$. Vortex breakdown crosses the trailing edge for Wings 8, 7, and 9 at approximately 18°, 19° and 20° angle-of-attack, respectively.

Wing 10. Fig. 6. The geometric data indicate that this wing is identical to Wing 8 except for a 10° bevel on the upper or leeward surface of the trailing edge. The two sets of data differ by up to 10% chord. Excluding an anomalous point at 26° angle-of-attack shows the data sets are shifted by about 5% chord or about 1° in angle-of-attack (the data from Wing 8 shows vortex breakdown forward of vortex breakdown on Wing 10). The data for Wing 10 follows the earlier prediction method of Huang and Hanff[1] over the centre of the wing, $0{\cdot}3 \le x/c \le 0{\cdot}9$, and is shifted downstream over the forward

https://doi.org/10.1017/S0001924000000294 Published online by Cambridge University Press

30% chord and upstream over the aft 10% chord. The data for Wings 8 and 10 lies on each side of the data for Wing 9 (same as Wing 8 with fuselage) indicating negligible effect of the fuselage.

Wing 11. Fig. 6. The fuselage is added to Wing 7 at the 0·684 chord position. This data agrees with the Huang and Hanff[1] prediction method over the entire range of angle-of-attack. The addition of the fuselage caused an upstream shift in vortex breakdown over the aft 20% chord. The data of Pelletier[9] is 10-15% chord upstream (forward) at the same angle-of-attack for his wing *A* with the symmetrical 10° bevel and fuselage.

Wing 13. Fig. 8. This wing is identical to Wing 8 (flat lower surface, 10° bevel on the upper surface leading edges, flat trailing edge) except one-half as thick. Vortex breakdown is about 10% chord upstream of its location on Wing 8 except near the trailing edge, $x/c \geq 0{\cdot}9$. This data agrees with the predictions of the Huang and Hanff[1] method for $x/c \leq 0{\cdot}7$ and deviates above this value (near the trailing edge).

Wing 14. Fig. 4. This is Wing 13 inverted (flat upper surface, 10° bevel on the lower surface, flat trailing edge). There is virtually no change in vortex breakdown location when the wing is inverted except for a slight upstream shift of 3-4% chord near the trailing edge, $x/c \geq 0{\cdot}8$. A comparison with the data of Wing 4 (twice as thick and bevelled at 45° on only the windward, lower surfaces, flat upper surface) shows the data agree from the trailing edge forward to $x/c = 0{\cdot}2$ where vortex breakdown is shifted downstream on the thicker wing, model 14-4.

5.0 CONCLUSIONS

For sharp-edged delta wings of 65° sweep In incompressible flow at zero roll and yaw angles:

(*i*) Empirical vortex-breakdown location methods do not sufficiently account for the wing's geometric details, particularly near the leading edge, to achieve accurate predictions.

(*ii*) The empirical prediction methods tend to agree as $\alpha \rightarrow 40°$ and vortex breakdown approaches the wing's apex. The experimental data also tend to the same limit.

(*iii*) Numerical solutions of the Navier-Stokes equations offer accurate prediction of vortex breakdown location for laminar flows. Experimental data scatter precludes a conclusion for turbulent flow.

(i*v*) In general. the addition of a symmetrically-disposed centre-body moves the vortex breakdown location aft, in the downstream direction.

(*v*) Increasing lower surface bevel angle tends to move vortex breakdown location aft.

(*vi*) The need for systematic data is emphasized but there are many, many variables with poorly understood effects that cause the published data to appear inconclusive and contradictory.

(*vii*) Wind tunnel wall effects corrections could account for some of the differences found.

ACKNOWLEDGMENTS

This work was conducted under a research programme of the US Air Force Office of Scientific Research. Sincere appreciation to X. Z. Huang, A. Pelletier and L. Traub for numerical data and N. G.Verhaagen for his helpful comments.

REFERENCES

1. HUANG, X.Z. and HANFF, E.S. Unsteady behavior of spiral leading-edge vortex breakdown, July 1996, AIAA Paper 96-3408, also Prediction of normal force on a delta wing rolling at high incidence, Aug 1993, AIAA 93-3686.
2. CIPOLLA, K.M. Structure of the Flow Past a Delta Wing with Variations in Roll Angle, May 1996, PhD dissertation, Lehigh University.
3. EARNSHAW, P.B. Measurements of vortex-breakdown position at low speed on a series of sharp-edged symmetrical models, November 1964, ARC CP No 828.
4. EARNSHAW, P.B. and LAWFORD, J.A. Low-speed wind-tunnel experiments on a series of sharp-edged delta wings, March 1964, ARC R&M No 3424.
5. GUGLIERI, G. and QUAGLIOTTI, F.B. Experimental investigation of vortex dynamics on delta wings, June 1992, AIAA Paper 92-2731. Also see GUGLIERI, G., ONORATO, M. and QUAGLIOTTI, F.B. Vortex breakdown study on a 65° delta wing tested in static and dynamic conditions, September 1992, ICAS 92-4.10.2, ICAS Proceedings, pp 2072-2081.
6. LAMBOURNE, N.C. and BRYER, D.W. The bursting of leading-edge vortices — some observations and discussion of the phenomena, April 1961, ARC R&M No. 3282.
7. LOWSON, M.V. and RILEY, A.J. Vortex breakdown control by delta wing geometry, *J Aircr*, 1995, **32**, (4), pp 832-838. Also see AIAA Paper 94-3487, August 1994.
8. PANTON, R.L. Effects of a contoured apex on vortex breakdown, *J Aircr*, 1993, **27**, (3), pp 285-288. Also see AIAA Paper 89-0193, January 1989.
9. PELLETIER, A. An Experimental Investigation of Vortex Breakdown on Slender Delta-Wing Planforms, April 1994, MSc thesis, University of Notre Dame. Also see PELLETIER, A. and NELSON, R.C. An experimental study of static and dynamic vortex breakdown on slender delta wing planforms, AIAA Paper 94-1879.
10. SKOW, A.M. and ERICKSON, G.E. Modern fighter aircraft design for high-angle-of-attack maneuvering, AGARD-LS-121, *High Angle-of-Attack Aerodynamics*, December 1982, pp 4-1 to 4-59. Also see ERICKSON, G.E. Vortex flow correlation, January 1981, AFWAL-TR-80-3143.
11. THOMPSON, D.H. A water tunnel study of vortex breakdown over wings with highly swept leading edges, May 1975, Note ARL/A 356, Australian Defence Scientific Service.
12. TRAUB, L.W. Simple prediction method for location of vortex breakdown on delta wings, *J Aircr*, 1996, **33**, (2), pp 452-454.
13. WENTZ, W.H. and KOHLMAN, D.L. Vortex breakdown on slender sharp-edged wings, July 1969, AIAA Paper 69-778. Also see *J Aircr*, 1971, **8**, (3), pp 156-161. See also Wind tunnel investigations of vortex breakdown on slender sharp-edged wings, November 1968, University of Kansas Report FRL 68-013, NASA CR 98737 also N69-14762.
14. HUANG, X.Z., SUN, Y.Z. and HANFF, E.S. Further investigations of leading-edge vortex breakdown over delta wings, June 1997, AIAA Paper 97-2263.
15. HUANG, X.Z., SUN, Y.Z. and HANFF, E.S. Circulation criterion to predict leading-edge vortex breakdown over delta wings, June 1997, AIAA Paper 97-2265.
16. TRAUB, L.W. Prediction of vortex breakdown and longitudinal characteristics of swept slender p1anforms, *J Aircr*, May-June 1997, **34**, (3), pp 353-359.
17. VERHAAGEN, N.G. Effect of sideslip on the flow over a 65-deg delta wing; preliminary report, December 1997, Delft University of Technology, The Netherlands.
18. ADDINGTON, G.A. The Role of Flow Field Structure in Determining the Aerodynamic Response of a Delta Wing, April, 1998, PhD dissertation, University of Notre Dame, Notre Dame, Indiana.
19. CHADERJIAN, N. and SCHIFF, L. Navier-Stokes prediction of a delta wing in roll with vortex breakdown, August 1993, AIAA Paper 93-3495.
20. GORDNIER, R.E. Numerical simulation of a 65 degree delta-wing flow-field, *J Aircr*, 1997, **34**, (4), pp 492-499. Also see AIAA Paper 95-0082, January 1995.
21. GURSUL, I. Unsteady flow phenomena over delta wings at high angle-of-attack, 1994, *AlAA J*, **32**, (2), pp 225-231.
22. HEMSCH, M.J., and LUCKRING, J.M. Connection between leading-edge sweep, vortex lift and vortex strength for delta wings, *J Aircr*, **27**, (5), pp 473-475.
23. VISSER, K.D. and NELSON, R.C. Measurements of circulation and vorticity in the leading-edge vortex of a delta wing, *AIAA J*, 1993, **31**, (1), pp 104-111.
24. JUMPER, E.J., NELSON, R.C. and CHEUNG, K. A simple criterion for vortex breakdown, January 1993, AIAA-93- 0866.
25. VISSER, K.D. and WASHBURN, A.E. Transition behavior on flat plate delta wings, June 1994, AIAA-94-1850- CP.

https://doi.org/10.1017/S0001924000000294 Published online by Cambridge University Press